Journal of Nano- and Electronic Physics
Vol. **18** No 3, 03031(10pp) (2026)

Журнал нано- та електронної фізики
Том **18** № 3, 03031(10cc) (2026)

REGULAR ARTICLE

OPEN ACCESS

Submillimeter-Wave InN Gunn Diodes Featuring a GaInN Graded-Gap Injector

I. Storozhenko[1,*], P. Sirenko[2]

[1] *State Biotechnological University, 61002 Kharkiv, Ukraine*
[2] *Riga Stradiņš University, LV-1007 Riga, Latvia*

(Received 29 March 2026; revised manuscript received 17 June 2026; published online 26 June 2026)

Developing efficient submillimeter-wave solid-state sources is a key challenge for semiconductor electronics. This study presents a theoretical investigation into high-frequency oscillations in submicron InN-based Gunn diodes featuring a graded GaInN injector near the cathode. The research employs a three-valley hydrodynamic electron transport model adapted for graded-gap III-nitride structures, accounting for coordinate-dependent parameters. This model is integrated into a self-consistent framework that couple's device equations with an equivalent resonant circuit and Poisson's equation. Unlike short-term simulations, this approach analyzes stable generation over thousands of cycles, providing realistic estimations of RF power, efficiency, and transients. Results show that the graded-gap GaInN injector significantly modifies space-charge wave dynamics, facilitating a transition from accumulation layer drift to dipole domain instability. Simulations demonstrate that optimizing the GaInN region length and composition substantially reduces the threshold electron concentration for current instability. An "incomplete domain drift" regime is identified, where space-charge layers dissipate within the active region before reaching the anode. This enables frequencies up to 391 GHz in a 1.0 μm device, surpassing frequencies of homogeneous InN structures. A diode with a 0.2 μm GaInN layer provides a peak power of 116.8 mW at 300.7 GHz, exceeding existing InGaAs and InP-based devices by orders of magnitude. The paper also addresses technological implementation challenges, including thermal management and the risk of impact ionization. It is demonstrated that InN-based diodes with a GaInN injector are potentially feasible and can be used to achieve oscillation in the sub-THz range.

Keywords: Gunn diode, Transferred Electron Device, Graded-gap semiconductor, Indium nitride, THz range, GaInN injector, Hot-electrons, NDR, Space-charge domains, Self-Oscillations

DOI: 10.21272/jnep.18(3).03031 PACS numbers: 85.30.Fg, 73.40.Kp, 72.20.Ht

1. INTRODUCTION

Despite the well-established advantages of submm-wave radiation, its practical implementation is hindered by a lack of compact solid-state sources, driving extensive research into both high-frequency transistors and the expansion of operating limits for conventional sources, such as transferred-electron devices (TEDs), avalanche transit-time (IMPATT) diodes, resonant-tunneling diodes (RTDs), frequency multipliers, and various vacuum devices [1-3].

This study aims to improve the performance of devices based on the transferred-electron effect (TEE). Several strategies have been proposed to increase the oscillation frequency in such structures. First, specialized cathode contacts such as metal-semiconductor junction, low-doped layer, heterojunction, graded-gap layer, and tunnel contact are employed to minimize the "dead zone". Although the underlying physics varies, these designs effectively reduce the distance required for electrons to acquire the energy necessary for intervalley transfer from the central to satellite valleys.

Since the oscillation frequency is governed by the dynamics of space-charge wave formation, transit, and quenching, an alternative approach involves using materials with higher electron mobility in high electric fields than traditional GaAs or InP [4-7]. In this regime, ballistic transport and velocity overshoot become critical. While materials such as InGaAs [8-11], InGaPAs [12], InAlAs [13], InPAs [14] and III-nitrides [15] have been investigated, they have yet to demonstrate a definitive advantage in attainable frequency over InP.

Currently, InP-based devices are the most efficient solid-state sources in the millimeter and submillimeter ranges. Specifically, InP Gunn diodes with a 1.1 μm active region and graded doping profiles have demonstrated substantial power extraction through harmonic generation: up to 3 mW at the second harmonic (300.5 GHz) and 23 μW at the third harmonic (455 GHz), with the fundamental frequency near 150 – 152 GHz [6,7]. Theoretical predictions further suggest that InP-based devices could remain viable for power extraction at frequencies approaching 500 GHz [7].

In contrast, fundamental-mode oscillations at 307.5 GHz have been reported in submicron (0.6 μm) planar $In_{0.53}Ga_{0.47}As$ Gunn diodes [10]. Since this frequency significantly exceeds the limits imposed by the steady-state drift velocity (0.7×10^7 to 0.9×10^7 cm/s), the performance is primarily attributed to the velocity overshoot effect, ballistic transport and local field en-

* Correspondence e-mail: prof.igor.storozhenko@gmail.com

Cite this article as: I. Storozhenko, et al., *J. Nano- Electron. Phys.* 18 No 3, 03031 (2026) https://doi.org/10.21272/jnep.18(3).03031

hancement at the n^+-n junction corners, which together accelerate the formation and transit of space-charge layers. However, the RF output power of such planar devices remains relatively low – approximately 28 μW [10] – compared to traditional InP structures.

These findings highlight that while InGaAs-based planar structures can reach higher fundamental frequencies due to ballistic effects, they still lag behind InP in terms of output power. This disparity underscores the need to explore alternative materials, such as III-nitrides, which combine high drift velocities with shorter electron relaxation times, potentially overcoming the power-frequency limitations of current technology.

Numerous theoretical studies suggest that GaN- and InN-based diodes could outperform GaAs and InP counterparts in both frequency and output power [15-30]. According to estimates presented in [17, 18], GaN possesses the potential for power generation at higher frequencies than both InN and AlN. Due to the inertia of intervalley electron transfer, the cutoff frequency is estimated at 3 THz for GaN and 2 THz for InN [17]. Additionally, the minimum electron drift velocity in GaN exceeds that of InN [17, 21]. However, the pronounced velocity overshoot effect in InN compensates for GaN's advantages when the active region length is reduced below 1 μm [17, 19, 20]. Numerical simulations [17-19] further indicate that InN diodes exhibit higher current oscillation amplitudes compared to their GaN counterparts. Current estimates place the operational cutoff frequency for both InN and GaN diodes within the 0.7-0.8 THz range.

Nevertheless, experimental realization of the Gunn effect in nitrides remains challenging. The primary challenge is that the oscillation regime in GaN and InN diodes is intrinsically associated with extremely high DC power levels. The threshold field for negative differential mobility (NDM) in GaN and InN is approximately 50 and 20 times higher than in GaAs, respectively, while drift velocities only double [21]. Furthermore, the formation of stable drifting domains in nitrides requires higher carrier concentrations in the active region [17-20]. This necessitates not only advanced thermal management to dissipate the resulting heat but also precise cathode engineering to facilitate rapid intervalley scattering. Traditional approaches used for GaAs and InP have proven largely ineffective for nitride-based structures.

Efforts to generate oscillations via intervalley electron transfer in GaN have primarily relied on various complex planar technologies [22-24], including the use of capping materials such as AlGaN [25], Ti/Al/Ti/Au/SiN (vertical architecture) [26], and boron nitride [27]. A second, less common approach involves the utilization of AlGaN-GaN heterojunctions [24, 28].

Despite these challenges, recent reports of first-time oscillation generation in GaN diodes within a 20 ns pulse [26,29] provide a basis for optimism. InN, in particular, is attractive due to its superior drift velocity [17-19, 21], though the potential for impact ionization to suppress the Gunn effect must be carefully considered [30].

In this paper, we investigate the generation of electrical oscillations in submicron (1 μm) InN-based Gunn diodes. We propose employing a compositionally graded InGaN region near the cathode to promote the nucleation of drifting domains, enhance RF output power, and lower the DC power consumption. The objective is to analyze the influence of the InGaN grading profile on space-charge wave dynamics and optimize the cathode region parameters for maximum efficiency in the sub-millimeter-range.

2. DEVICE PARAMETERS AND SIMULATION METHODOLOGY

2.1 Device Parameters

The schematic of the n^+– n – n^+ InN -based Gunn diode featuring a near-cathode compositionally $Ga_{1-x(z)}In_{x(z)}N$ graded-gap layer is shown in Fig. 1.

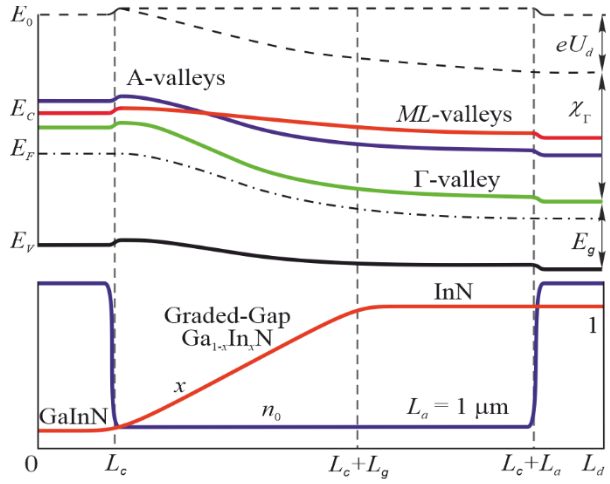

Fig. 1 – Band diagram, doping profile, and InN mole fraction of an InN diode with a graded-gap GaInN layer.

The structure consists of an n^+- $Ga_{1-x}In_xN$ (x = 0–1) cathode, an n^+-InN anode, and an active region situated between them. The active region incorporates an n type graded-gap $Ga_{1-x}In_xN$ layer, where the InN mole fraction x increases from the cathode interface (x = 0–1) to x = 1 at the anode side over a grading length L_g. This length L_g was varied from 10 nm up to the full length of the active region.

The lengths of the cathode and anode regions are 0.4 μm each, while the active region length is L_a = 1.0 μm. The doping concentration in the n^+ contact layers is 10^{18} cm^{-3}, and the electron concentration in the active region was varied within the range of 5×10^{16} to 1.1×10^{17} cm^{-3}. The device cross-sectional area is S = 400 μm^2. The material model for $Ga_{1-x}In_xN$ assumes a wurtzite crystal structure with Γ, M-L, and A conduction band valleys. The InN mole fraction follows an S-shaped distribution, consistent with the methodology in [12].

2.2 Electron Transport Model

We investigate the process of oscillation generation using a hydrodynamic model of electron transport in a graded-gap semiconductor. The model is based on the solution of the Boltzmann kinetic equation assuming that electrons obey a shifted Maxwellian distribution. It represents a system of equations consisting of continuity equations, current density equations, and energy balance equations for each of the three non-equivalent conduction-band valleys of the semiconductor, as well as the Poisson equation [12, 31].

The model is adapted for graded-gap semiconductors. The current density equations incorporate additional terms including the spatial derivatives of the electron affinity, the energy gap between valleys, and the effective mass. Furthermore, all relaxation times in the graded-gap semiconductor depend on the coordinate due to the coordinate dependence of all semiconductor parameters. The model is explained in detail in [12, 31]. This system of equations is solved numerically. The differential equations are approximated by finite-difference equations. Each of these is reduced to a system of algebraic equations and solved using the Thomas algorithm.

All processes are considered only along the z-coordinate. We assumed that only an external electric field acts on the semiconductor. The lattice temperature is assumed to be constant at 300 K. The average current density in the device is defined as the sum of the average electron conduction currents and the displacement current.

This model accurately captures the qualitative physics of space-charge wave nucleation and drift. It allows for the study of the process over a long period of time, which is crucial for investigating the oscillation generation when the diode is placed in a resonator. We studied oscillations in the diode both with and without a resonator. If the resonator is absent, the voltage U is applied directly to the diode. When placed in a resonator, unlike simplified models with a fixed harmonic voltage, we utilize a self-consistent system of equations for the diode and an equivalent resonant circuit. This approach provides a realistic estimation of the output power and efficiency, accounting for the influence of the external circuit.

2.3 Self-Consistent Circuit Integration

The placement of the diode within a resonator is modeled by an equivalent circuit connecting the device to a parallel RLC resonant circuit, as shown in Fig. 2.

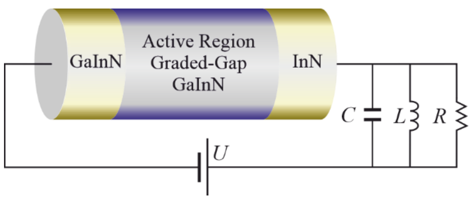

Fig. 2 – Equivalent circuit of the generator: Gunn diode, DC bias source, and RLC resonator.

In this case, the voltage applied to the diode is $U_d(t) = U - U_c(t)$, where U_c is the voltage drop across the oscillatory circuit:

$$C\frac{dU_c}{dt} + \frac{1}{L}\int_0^t U_c dt + \frac{1}{R}U_c = SJ_d(t).$$

The integro-differential equation for the resonant circuit is solved numerically in conjunction with the system of electron transport equations for the Gunn diode. The instantaneous oscillation power in the resonant circuit is determined as $P(t) = J_d(t)U_c(t)S$.

The input data include the applied DC voltage U, the doping level, the InN mole fraction, and the diode geometry parameters. The model incorporates the quality factor Q and the resonant frequency f along with the semiconductor material parameters [15, 17]. The equivalent inductance of the resonator is determined by the resonant frequency as $L(f) = \rho \cdot \omega^{-1}$, where the characteristic impedance is fixed at $\rho \approx 4.7\ \Omega$ (corresponding to $L = 2.5$ pH at 300 GHz). This relationship ensures electrodynamic scaling of the resonator parameters across the sub-THz range. Such parameters are physically consistent with Whispering Gallery Mode (WGM) resonators, which maintain high Q-factors in this frequency range. In this context, the equivalent inductance $L(f)$ represents the effective reactive coupling between the Gunn diode and the resonator. The equivalent capacitance and conductance are then calculated based on Q, f, and L according to classical linear circuit theory.

The output data consist of the dynamic distributions of electron concentration, energy, current density, and electric field intensity. We investigated the oscillation spectra of current and power for InN diodes at various graded-layer lengths, electron concentrations in the active zone, InN mole fractions in the GaInN alloy, applied voltages, and resonant frequencies.

To ensure the numerical stability and accuracy of the spectral characteristics, the simulation is carried out for 4 ns (over 1200 oscillation periods). This observation interval is initiated only after an initial transient phase of several hundred cycles, during which the oscillation amplitude and phase reach a steady-state regime. It was established that further increasing the number of periods leads to negligible changes in the output power and frequency, confirming the statistical reliability of the obtained results.

3. RESULTS OF THE RESEARCH

3.1 Self-Sustained Current Oscillations

Short relaxation times in InN [17, 21, 33] enable the generation of self-sustained oscillations in diode with an active region length of 1 μm. The electron concentration is the key parameter determining the threshold for the onset of current oscillations. For a diode with the given geometry, generation is achieved at a doping level of at least 8.4×10^{16} cm^{-3} (Fig. 3, curve 1). The increase in oscillation frequency observed when the electron concentration decreases is due to the enhancement of electron mobility resulting from reduced scattering on ionized impurities.

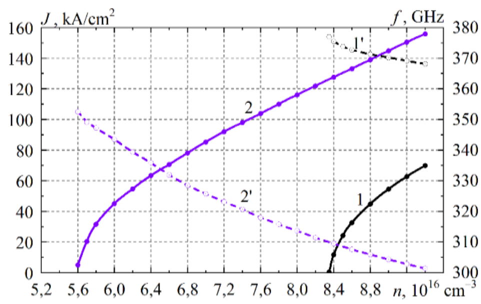

Fig. 3 – Amplitude (solid lines) and frequency (dashed lines) of the fundamental current density harmonic vs. electron concentration in the diode active region: 1 — InN diode; 2 — InN diode with a 0.1 μm GaN–InN graded-gap layer

According to estimates in [19], the Kroemer criterion for InN is $n \cdot l_a = 2.1 \times 10^{12}$ cm^{-2}, while estimates in [17] suggest $n \cdot l_a = 3.81 \times 10^{12}$ cm^{-2}. This implies that for the onset of current instability associated with electric domain drift, the electron concentration in the active region should be at least $2.1 \times 10^{16} \ldots 3.8 \times 10^{16}$ cm^{-3}. However, our simulation results indicate that undamped self-sustained oscillations in the InN diode only become possible at an electron concentration in the active region of at least 8.4×10^{16} cm^{-3}. This value is not a revised Kroemer criterion but represents the threshold for autonomous instability without an external resonator. The cause of current oscillations in the InN diode (Fig. 4, curve 1) is the drift of an accumulation layer. The leading edge of the traveling space-charge wave is not depleted of charge carriers (Fig. 5).

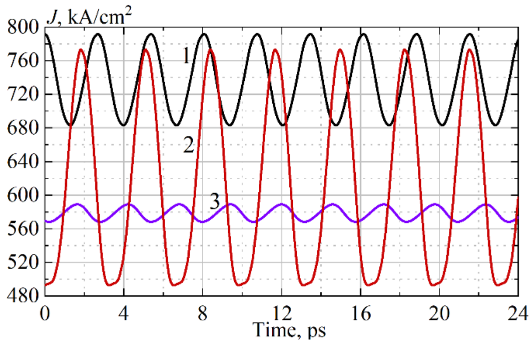

Fig. 4 – Current density self-oscillations: 1 – InN diode, U = 18 V (f = 371 GHz); 2 – 0.2 μm graded-gap GaN-InN diode, U = 23 V (f = 304 GHz); 3 – 0.4 μm graded-gap GaN-InN diode U = 12.7 V (f = 385 GHz).

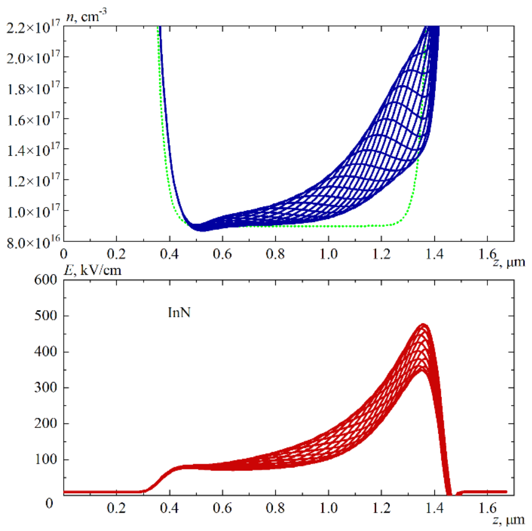

Fig. 5– Spatio-temporal distributions of electron density and electric field during one oscillation period (371 GHz) in an InN diode at a bias voltage of 18 V

For comparison, undamped self-oscillations at this concentration do not occur in GaN [19, 22, 24, 25] and GaAs diodes [12]. The application of a GaN GaN-InN InN graded-gap in the near-cathode region initiates a dipole instability (Fig. 6). The space-charge distribution shows that the leading edge of the wave is depleted of carriers, which is a characteristic feature of domain formation. The presence of the dipole instability accounts for the higher amplitude and lower frequency of the current density self-oscillations (Fig. 4, curve 2) compared to homogeneous InN diode. The threshold electron concentration in the active region for the structure with a graded layer $L_g = 0.1$ μm is 5.6×10^{16} cm^{-3} (Fig. 3, curve 2).

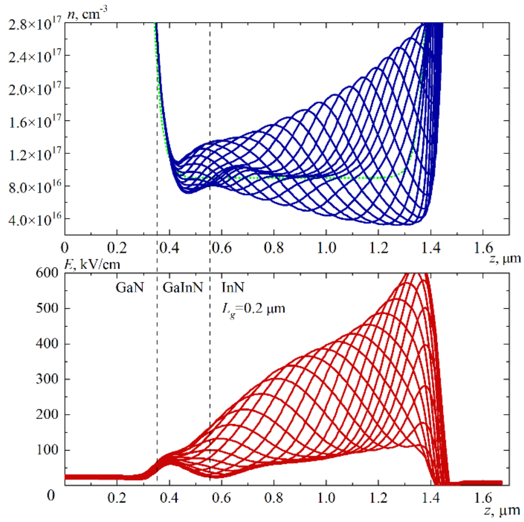

Fig. 6 – Spatio-temporal distributions of electron density and electric field during one oscillation period (304 GHz) in a 0.2 μm graded-gap layer GaN-InN diode at a bias voltage of 23 V

For systematic simulation and analysis of the generation processes, an electron concentration of 9.0×10^{16} cm^{-3} was selected. At this doping level, which exceeds the threshold value, the InN diode exhibits a sustained self-oscillation mode. This enables a consistent comparative analysis of the dynamic characteristics of structures both with and without the GaInN graded-gap layer.

Sustainable current generation in the homogeneous InN diode is observed in the applied voltage range from 13.5 to 24.5 V (Fig. 7, curve 1). The generation process exhibits high sensitivity to the external bias. An increase in voltage leads to a reduction in the oscillation frequency decreases from 376 to 364 GHz. This is due to the fact that space-charge waves do not reach full formation over the length of the active region. Higher applied voltage causes more intensive electron transfer to the satellite valleys in the drift instability region. Consequently, the electron concentration in the satellite valleys increases and the average drift velocity of the charge instability from cathode to anode decreases. The maximum amplitude of the fundamental harmonic of the current density is 54.5 kA/cm^2 and is achieved at a bias voltage of 18 V which corresponds to an oscillation frequency of 370 GHz.

The introduction of a GaInN graded-gap layer into the active region near the cathode improves the conditions for space-charge wave formation in the diode. As a result, the current oscillation amplitude increases (Fig. 7, curve 2-4). The reasons for such influence of the graded-gap semiconductor on the generation process are discussed in detail in [9, 12]. The electron mobility in the Γ-valley and the energy gap between the central and the nearest satellite valleys of the conduction band within the graded layer exert the most significant influence on the space-charge wave formation. These factors determine the intensity of the satellite valley population. In the GaInN layer the electron mobility and the energy gap decrease as the GaN mole fraction increases.

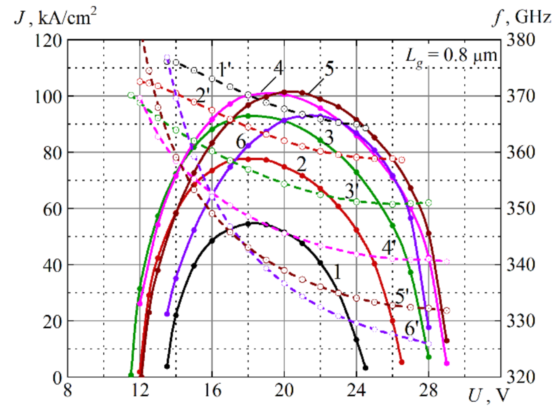

Fig. 7 – Amplitude (solid) and frequency (dashed) of the fundamental current density harmonic vs. voltage for an InN diode with a 0.8 μm $Ga_{1-x}In_xN$ graded-gap layer. In content x: 1 – 1 (InN); 2 – 0.8; 3 – 0.6; 4 – 0.4; 5 – 0.2; 6 – 0 (GaN).

The amplitude and frequency of the fundamental current oscillation harmonic in a diode with a graded-gap layer near the cathode depend on the length and composition of this layer. To study these dependencies, we simulated an InN diode with a GaInN graded-gap layer of various lengths and different InN mole fractions in the alloy. Figs. 7-10 shows the dependencies of the amplitude and frequency of the fundamental current density oscillation harmonic on the applied DC voltage for different graded-gap layer lengths and different InN content in the cathode region.

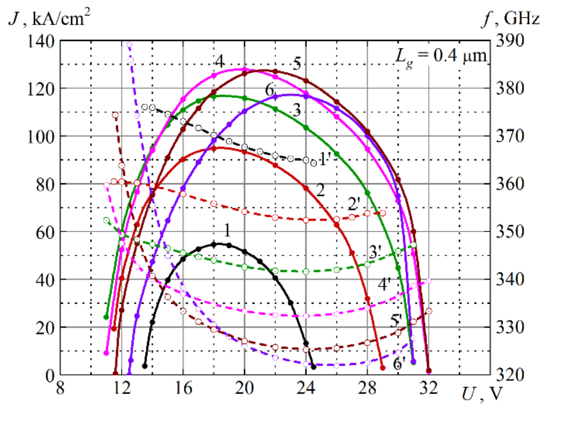

Fig. 8 Amplitude (solid) and frequency (dashed) of the fundamental current density harmonic vs. voltage for an InN diode with a 0.4 μm $Ga_{1-x}In_xN$ graded-gap layer. In content x: 1 – 1 (InN); 2 – 0.8; 3 – 0.6; 4 – 0.4; 5 – 0.2; 6 – 0 (GaN)

Analysis of these dependencies reveals several patterns. There is an optimal composition of the GaInN graded-gap alloy at which the electric current density oscillation amplitude is maximal. This optimum depends on the length of the graded-gap layer. The shorter the graded-gap layer length, the lower the InN mole fraction in GaInN required for the optimum. For example, when L_g ranges from 0.4 to 0.8 μm the highest current density oscillation amplitude is achieved at 60-80 % of InN in the GaInN layer (Figs. 7, 8). If L_g is between 0.1 and 0.2 μm the GaN-InN composition becomes optimal (Figs. 9, 10). The largest amplitude of the fundamental current density oscillation harmonic is 144.8 kA/cm² at a frequency of 304.4 GHz in the GaN-InN diode with a graded-gap layer length of 0.2 μm and an applied DC voltage of 23 V (Fig. 9, curve 6).

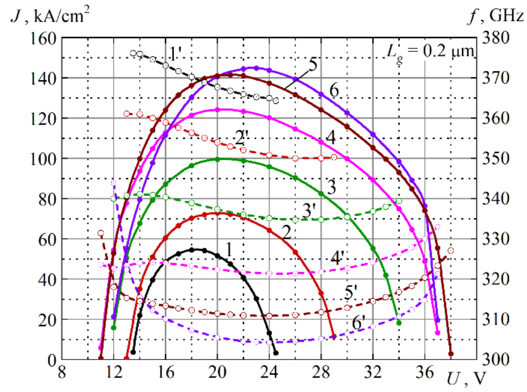

Fig. 9 – Amplitude (solid) and frequency (dashed) of the fundamental current density harmonic vs. voltage for an InN diode with a 0.2 μm $Ga_{1-x}In_xN$ graded-gap layer. In content x: 1 – 1 (InN); 2 – 0.8; 3 – 0.6; 4 – 0.4; 5 – 0.2; 6 – 0 (GaN)

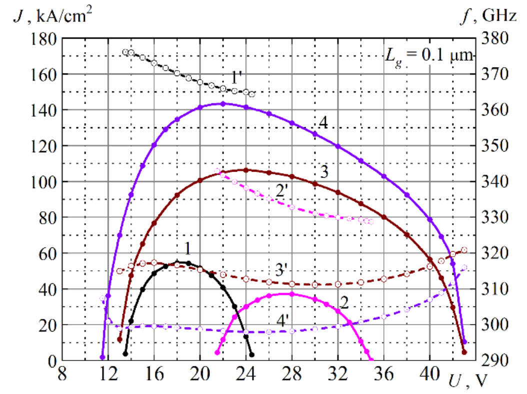

Fig. 10 – Amplitude (solid) and frequency (dashed) of the fundamental current density harmonic vs. voltage for an InN diode with a 0.1 μm $Ga_{1-x}In_xN$ graded-gap layer. In content x: 1 – 1 (InN); 2 – 0.4; 3 – 0.2; 4– 0 (GaN)

Diodes with a long GaInN-InN graded-gap layer (0.2-0.8 μm) exhibit a specific effect that is absent in homogeneous diodes. The physical nature of this effect lies in the formation of an incomplete domain with a spatially limited lifetime. At low applied DC voltages, space-charge waves drift only a short distance within the active region. This occurs because the conditions for the formation and drift of space-charge waves in a graded-gap semiconductor vary with the coordinate. Near the cathode, the semiconductor composition creates an electron concentration inhomogeneity. This inhomogeneity begins to grow and drift through the graded-gap semiconductor toward the anode. At a certain distance from the cathode, the semiconductor composition changes such that the space charge stops growing and begins to dissipate. Consequently, the charge instability dissipates before reaching the anode (Fig. 11).

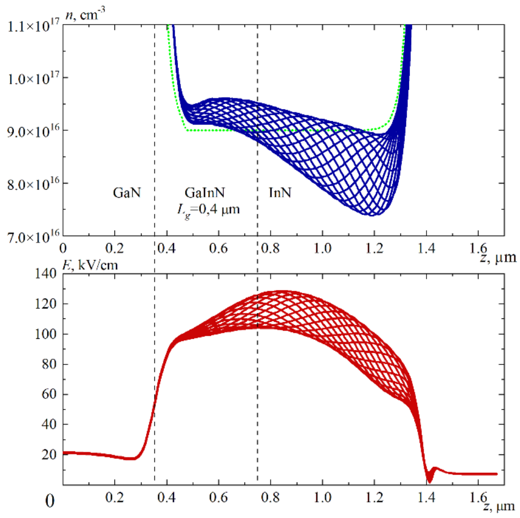

Fig. 11 – Spatio-temporal distributions of electron density and electric field during one oscillation period (385 GHz) in a 0.4 μm graded-gap layer GaN-InN diode at a bias voltage of 12.7 V

At low applied voltages, the oscillation frequency is high and can exceed the self-oscillation frequency of a homogeneous InN diode (Fig. 4, curve 3). This effect is observed as a sharp decrease in the oscillation frequency with increasing bias voltage (Figs. 7, 8). The frequency decreases because an increase in the applied voltage extends the region where the charge instability sequentially forms, drifts, and dissipates.

The widest frequency range is achieved in a diode with a 0.4 μm GaN-InN graded-gap layer. At 12.5 V, the fundamental harmonic frequency is 389 GHz, and at 26 V, it reaches a minimum value of 321.9 GHz (Fig. 8, curve 6'). A further increase in the applied voltage leads to a slight increase in frequency until the generation vanishes. This frequency growth is associated with an increase in the average domain velocity at a fixed transit length, which in this mode becomes equal to the distance between the cathode and the anode.

In the diode with a 0.8 μm GaN-InN graded-gap layer, the frequency range width is slightly smaller than that for the 0.4 μm layer, ranging from 376.9 to 325.9 GHz (Fig. 7). This effect weakens as the graded-gap layer length decreases (Figs. 9, 10). If the graded-gap layer length is 0.1 μm, the oscillation frequency almost ceases to depend on the applied voltage (Fig. 10, curves 3' and 4').

Self-oscillations do not occur in the diode with a short graded-gap layer L_g= 0.1 μm if the InN mole fraction in GaInN is within the 50-90 % range. In Fig. 10, the curves corresponding to $Ga_{0.2}In_{0.8}N$-InN and $Ga_{0.4}In_{0.6}N$-InN diodes are absent because self-oscillations do not arise at any applied voltage.

Reducing the length of the graded-gap layer increases the width of the voltage range where the diode generates current oscillations. For example, a diode with a 0.8 μm GaN-InN graded-gap layer exhibits active properties in the voltage range from 13.5 to 28 V (Fig. 7, curve 6). If the GaN-InN layer length is 0.1 μm, the operating voltage range is from 11.5 to 43 V.

Thus, to obtain current oscillations with the maximum frequency of 375-390 GHz, which exceeds the InN diode oscillation frequency, a 0.4 μm GaN-InN graded-gap layer and a threshold low bias voltage of 12.5-13 V should be used. In this case, the generation efficiency is expected to be very low since only a small part of the active region participates in the oscillation generation. At the same time, low DC power consumption is also expected.

On the other hand, to generate current oscillations with the maximum amplitude of 144.8 kA/cm^2 at a frequency of 304-305 GHz, a diode with a 0.2 μm GaN-InN layer and a bias voltage of 22-24 V should be used.

The InN diode with a GaInN graded-gap layer is capable of generating sustained self-oscillations at a lower electron concentration than the InN diode. If the electron concentration decreases, the oscillation power reduces, while their frequency increases.

3.2 Oscillation Generation in a Resonator

Placing the diode into a resonator significantly alters its characteristics. In this case, the structure is subjected to a high-frequency electric field. The frequency of these oscillations is determined by both the current dynamics within the diode and the parameters of the resonator itself.

We considered the case of a high-Q resonator ($Q = 10^3$). The selection of specific semiconductor composition profiles was based on the self-oscillation characteristics providing the highest frequency or current amplitude.

Fig. 12 shows the oscillation power versus frequency for increasing bias voltages. The frequency decreases as the voltage rises. For each bias point, the resonator was tuned to maximize output power. The resulting power peaks occur at frequencies slightly offset from the diode's free-running oscillation points.

The dependence of oscillation power on frequency in the homogeneous InN diode is nearly symmetric with respect to 363.8 GHz (Fig. 12, curve 1). However, in the graded-gap structures, this dependence becomes significantly asymmetric as the layer length decreases and the GaN mole fraction increases (Fig. 12, curves 2-5). Such asymmetry is caused by the non-linear and non-monotonic behavior of the oscillation frequency as a function of the applied voltage. Unlike the typical nearly linear decrease, the frequency dependence in these structures becomes non-linear, and for short graded-gap layers, it reaches a minimum and begins to increase at voltages above the optimal value (Fig. 8, 9, curves 2'-6'). Consequently, the peak of the power-frequency characteristic shifts toward the minimum generation frequency, resulting in a pronounced positive asymmetry (right-skewed) of the characteristic.

The maximum RF power of the homogeneous InN diode is 42.3 mW at 363.8 GHz with an applied voltage of 18 V. The DC power consumption is 52.3 W, and the operating frequency range spans from 351 to 376.5 GHz.

The highest oscillation frequency of 393.1 GHz was observed in the InN diode with a L_g =0.4 μm GaN-InN graded-gap layer at 12.4 V (Fig. 12, curve 4). The oscillation power was 21.8 μW, and the DC power consumption was 28.7 W. The frequency range for this structure is 323.4-393.1 GHz. The diode reaches a peak power of 61.4 mW at 318.3 GHz and 24 V (DC power consumption of 55.4 W).

The highest peak oscillation power of 116.8 mW at 300.7 GHz was achieved in the InN diode with a L_g =0.2 μm GaN-InN graded-gap layer at an applied voltage of 22 V (Fig. 12, curve 5). The DC power consumption in this mode is 53.3 W.

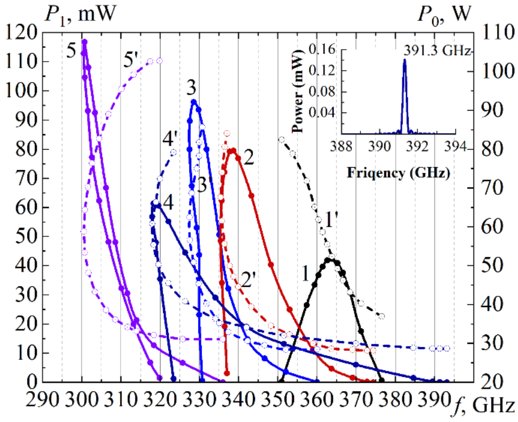

Fig. 12 – RF power P_1 (solid) and DC power P_0 (dashed) vs. frequency for various diodes in a resonator ($Q = 10^3$): 1 – InN; 2 – $Ga_{0.4}In_{0.6}N$-InN, $L_g = 0.6$ μm; 3 – $Ga_{0.4}In_{0.6}N$-InN, $L_g = 0.4$ μm; 4 – GaN-InN, $L_g = 0.4$ μm; 5 – GaN-InN, $L_g = 0.2$ μm. The inset shows the power spectrum

4. DISCUSSION OF RESULTS

4.1 Physical Mechanisms of RF Power and Frequency Enhancement

Optimization of the graded-gap layer length and composition allows for a reduction in the critical electron concentration, an increase in peak oscillation power, and an enhancement of the generation frequency. The power increase is attributed to the onset of domain instability. The frequency enhancement occurs due to the "incomplete domain drift" effect. In this mode, the forming domain does not drift across the entire length of the active region but only through the portion adjacent to the cathode. The length of this transit region depends on the voltage applied to the diode. An increase in voltage leads to an expansion of the transit region and a corresponding decrease in frequency. We have demonstrated that in structures with a graded-gap layer, the domain does not necessarily have to dissipate at the anode; under certain conditions, it can dissipate within the active region itself. The graded-gap cathode initiates domain formation, and this mechanism enables a peak frequency of 391 GHz for a device with a total length of 1 μm.

4.2 Thermal Management Challenges

The issue of high DC power dissipation in homogeneous InN diodes remains unresolved. The introduction of a graded-gap layer does not fully eliminate this drawback. In the peak RF power generation mode, the DC power consumption levels for both diode types are comparable. At optimal frequency and voltage, the DC power of the homogeneous diode is 42.3 W, while for the diode with a graded-gap layer (L_g =0.2 μm), this value reaches 53.3 W.

Given a cross-sectional area of 400 μm², the power density ranges from 10.6 to 13.3 MW/cm². A straightforward estimation based on the thermal resistance of the active layer and the thermal conductivity of InN (≈ 45 W/(m·K)) indicates that at such heat flux densities, the steady-state temperature rise would several times exceed the thermal decomposition threshold of InN (over 800 K). This precludes the operation of the device in continuous-wave mode without the implementation of extreme cooling solutions.

Despite the thermal constraints, the use of a graded-gap layer offers several significant advantages. First, the peak power of such a diode is nearly three times higher than that of its homogeneous counterpart. This provides a performance margin that allows for a reduction in DC power consumption by lowering the bias voltage while maintaining the required output signal level. Second, the graded-gap layer enables a 33 % reduction *i-n* the critical electron concentration within the active region. Utilizing a lower concentration provides two key benefits:

i) A further reduction in consumed DC power, which facilitates heat dissipation;

ii) An increase in the generation frequency.

Consequently, optimizing the carrier concentration helps to partially offset the high current density inherent in the maximum power mode.

In GaInN-InN diodes, the "incomplete domain drift" mode emerges at the lowest possible threshold voltages. In this mode, the DC power consumption is 28.7 W, which is 25 % lower than the minimum power of a homogeneous diode. For a cross-sectional area of 400 μm² and a voltage of 12.4 V, the current density reaches 578.6 kA/cm². The power density in this "mild" mode is 7.17 MW/cm². Despite the reduction, such a load remains extreme, which is still significantly above the thermal stability threshold of the material.

Reducing device cross-section fails to mitigate overheating, as thermal resistance increases proportionally with power reduction, leaving the operating temperature unchanged. Conversely, a planar geometry offers superior thermal management. The active region contacts a high-conductivity substrate (e.g., diamond, BN, or AlN) across its entire lateral surface. Efficiency can be further enhanced by top-surface encapsulation with similar materials. While this dual-cooling approach ensures stable operation at 12.7 V, the reduced active volume inherently limits the absolute RF power, a trade-off for high-signal applications.

The use of a pulsed mode can, to some extent, prevent the thermal destruction of the device. In the nanosecond range (10^{-9} to 10^{-8} s), the heating is essentially adiabatic. Due to the finite rate of thermal diffusion, the energy generated during the pulse has insufficient time to dissipate into the substrate. However, owing to the short pulse duration, the total accumulated heat is expected to remain below the InN thermal decomposition threshold (800 K). Estimations indicate that in the "mild" mode (P_{dc} =28.7 W), the time required for the temperature to reach this critical point is approximately 14 ns

Nevertheless, even before reaching the decomposition threshold, significant heating of the active region (up to 600-700 K) substantially affects the oscillation conditions. The temperature rise leads to a narrowing of the bandgap and a reduction in the energy gap between conduction band valleys. This alters the conditions for intervalley electron transfer and reduces the efficiency of space-charge wave formation. Consequently, short-pulse operation is essential not only for maintaining the structural integrity but also for minimizing the thermal drift of the device's frequency and power characteristics.

To reduce the operating temperature, substrates with maximum thermal conductivity, such as diamond or AlN, must be employed. The epitaxial growth of InN on such substrates is technically feasible and provides a primary path for heat removal. However, external heat sinking alone is insufficient to suppress extreme heat fluxes. The fundamental limitation lies in the finite rate of energy transfer from the electronic subsystem to the crystal lattice, followed by slow thermal diffusion through the InN layer itself to the substrate interface.

To address this, we propose using hot-electron extraction channels [32]. This method enables the removal of high-energy carriers from the active region before they transfer their energy to the lattice via phonon scattering. Such a "ballistic cooling" mechanism reduces direct lattice heating from within.

Further efficiency can be achieved by incorporating 2D layers (e.g., h-BN) to redistribute heat fluxes and prevent local hotspots [27]. The concept of using "energy filters" for active region cooling via ballistic energy extraction [32], combined with diamond heat sinks, is expected to enable the stabilization of InN diode operation even at extreme current densities. This could potentially provide a foundation for transitioning from nanosecond pulses to longer duty cycles.

4.3 The Role of Velocity Overshoot and Model Limitations

When interpreting the results, it should be noted that the hydrodynamic model employed accounts for the velocity overshoot effect only partially. This is due to the reliance on the Maxwellian distribution function for averaging the Boltzmann transport equation, which does not fully capture the distribution asymmetry or the contribution of high-energy ("hot") electrons.

Indium nitride exhibits unique transport properties: high mobility (up to 4000 $cm^2/V\cdot s$) and a substantial intervalley energy gap (1.7-1.8 eV). These factors create conditions for extreme velocity overshoot, where peak electron velocities can reach 108 cm/s before the onset of intense intervalley scattering. The overshoot region length in InN is estimated at 0.5-0.8 μm, which is comparable to the active zone dimensions of the studied diodes.

It is crucial to emphasize that the previously proposed hot-electron extraction channels synergistically complement this effect. By removing energy near the anode, lattice heating is minimized, which increases the mean free path of electrons and enables the fullest realization of ballistic transport.

The current model, which does not fully account for band non-parabolicity and extreme overshoot, provides what is effectively a lower limit for both frequency and power. The obtained values of 320-391 GHz are a conservative estimate. In a real device, due to higher average carrier velocities, operating frequencies could reach 450 GHz. However, since the primary objective of this work is to study the influence of the graded-gap profile on space-charge wave dynamics rather than the precision refinement of InN material parameters, the standard hydrodynamic model is deemed an effective tool that reliably conveys the qualitative physics of the processes.

4.4 Impact Ionization

There is another critical factor that can limit the efficiency of InN Gunn diodes. In indium nitride, there is a probability of overlap between the energy thresholds for intervalley transfer and band-to-band impact ionization. Under electron gas heating conditions, the velocity overshoot effect may increase the probability of impact ionization events before carriers transfer to the satellite valleys. The increase in lattice temperature and the associated bandgap narrowing reduce the ionization energy threshold.

At the optimal voltage applied to the diode, the peak electric fields in the domain (for the InN diode with a graded-gap layer) or the accumulation layer (for the homogeneous diode) can reach 500-600 kV/cm at certain brief moments in time (Figs. 5 and 6). It should be noted that a precise experimental determination of the fundamental impact ionization threshold in InN remains challenging, as samples often undergo premature destruction at significantly lower fields (300-400 kV/cm) due to high background carrier concentrations and thermal effects. Theoretical studies using the ensemble Monte Carlo method [33] provide a more robust basis for analysis, indicating that intervalley scattering remains the dominant energy relaxation mechanism at field intensities up to at least 500-600 kV/cm. This suggests that electrons are scattered into upper valleys with higher effective masses before they can accumulate sufficient kinetic energy to trigger an ionization avalanche.

Furthermore, in GaInN-InN diodes operating in the 'incomplete domain drift' mode, which emerges at the lowest possible threshold voltages, the peak electric field reaches only approximately 130 kV/cm. This value is substantially lower than even the most conservative estimates for the onset of impact ionization. Consequently, this mode of operation offers an additional margin of stability, virtually eliminating the probability of impact ionization overlapping with intervalley transfer and ensuring the reliable realization of the Gunn effect in the submicron structures studied

4.5 Technological Implementation

The fabrication of an ideal GaInN-InN graded-gap layer with a length of 0.2-0.6 μm. presents certain technological challenges. The epitaxial growth of a wide-bandgap GaN-based layer on an InN active region is complicated by a significant lattice mismatch of approximately 11 %. However, since the primary function of this layer is the local reduction of electron mobility to facilitate domain nucleation, the presence of structural defects originating from this mismatch is considered acceptable. In practice, the smooth compositional profile assumed in our model can be replaced by a stepwise change in Ga concentration using a digital alloy or a superlattice structure. Such a discrete approximation of a continuous profile is a standard and effective practice in THz diode design.

Another limitation is the deposition temperature of GaN, which is significantly higher than the thermal degradation temperature of InN. Traditional GaN growth at 1000 °C would lead to the destruction of the underlying InN layer. This issue is addressed by using low-temperature growth methods, such as molecular beam epitaxy or plasma-enhanced atomic layer deposition. At temperatures of 400-500 °C, it is possible to form GaN or GaInN layers without loss of interface quality. Although such layers have a higher defect density, they fully perform their function of local mobility reduction for domain formation.

4.6 Comparison with State-of-the-Art

The performance of the proposed InN diodes was compared with experimental data for InP and InGaAs counterparts [6, 7, 11]. Specifically, InP Gunn diodes with a 1.1 μm active region and graded doping delivered 150-152 GHz at the fundamental mode, while their second (300.5 GHz) and third (455 GHz) harmonics reached power levels of 3 mW and 23 μW, respectively [6, 7]. In contrast, our InN graded-gap device provides fundamental-mode generation at 301 GHz with an output power of 116.8 mW, which is over an order of magnitude higher than the second-harmonic power of InP diodes at the same frequency.

Furthermore, compared to submicron (0.6 μm) planar InGaAs/InP diodes, which report a maximum of 28 μW for oscillations above 300 GHz [11], our vertical graded-gap structure demonstrates a power superiority of several orders of magnitude. These results confirm that utilizing graded GaInN transitions is an effective strategy for advancing Gunn effect sources into the submillimeter range without the efficiency losses inherent in frequency multiplication.

4.7 Methodological Features of the Simulation

The mathematical model is specifically tailored for transport phenomena in graded-gap structures based on balance equations derived by averaging the Boltzmann transport equation. We employ the shifted Maxwellian distribution approximation for the electron gas within each of the three non-equivalent valleys. This approach enables a self-consistent description of the mean energy (electron temperature) and drift velocity dynamics for each valley separately.

Such a framework ensures a rigorous treatment of the internal quasi-electric fields arising from compositional gradients. These fields, which originate from the spatial dependence of electron affinity, inter-valley energy gaps, and effective masses, are incorporated into the current density equations through corresponding spatial derivatives [12, 17]. Furthermore, the model accounts for the coordinate dependence of all relaxation times, as determined by the local variation of semiconductor parameters along the graded layer.

In contrast to conventional methods employing a fixed harmonic voltage, this work implements a self-consistent coupling between the electron transport equations and the external resonant circuit. This accounts for the dynamic voltage redistribution between the active device and circuit elements, bringing the numerical experiment closer to real physical measurement conditions. To ensure spectral reliability, the system was analyzed over a 4 ns interval (exceeding 1200 oscillation periods) following the stabilization of transients, confirming both frequency precision and the temporal stability of the "incomplete domain drift" mode.

5. CONCLUSIONS

This study employs a self-consistent integration of electron transport and resonant circuit equations, providing a realistic estimation of RF power and efficiency. The investigation reveals that GaInN graded-gap layers are decisive for enhancing InN-based Gunn diode performance. Specifically, the graded transition facilitates a shift in space-charge dynamics from accumulation layer drift to dipole domain formation, significantly increasing oscillation amplitude and enabling robust frequency tuning in the submillimeter rang.

Optimization of the graded-gap region allows for a stable generation regime at doping levels approximately 33% lower than those required for homogeneous structures. A key finding is the identification of the 'incomplete domain drift' effect, where the instability dissipates before reaching the anode, allowing the device to overcome transit-time limitations and reach a peak frequency of 391 GHz. Comparative analysis indicates that our vertical InN diodes offer a substantial power advantage, with a predicted 116.8 mW at 300.7 GHz, significantly exceeding traditional InP and InGaAs sources operating in harmonic modes. While peak internal fields approach the impact ionization threshold, the graded-gap profile helps manage the field distribution and mitigates the risk of premature breakdown.

Despite these advantages, extreme DC power densities (10.6-13.3 MW/cm²) necessitate nanosecond pulse operation and advanced thermal management, such as diamond heat sinks, to prevent InN thermal decomposition. These results provide a physical framework for next-generation nitride oscillators, bridging the gap between electronic and photonic THz sources. Future research should focus on Monte Carlo refinement of velocity overshoot and further reduction of doping concentrations to minimize power consumption.

REFERENCES

1. R.J. Trew, *IEEE Trans. Electron Dev.* **52** No 5, 638 (2005) https://doi.org/10.1109/TED.2005.845862.
2. K. Sengupta, T. Nagatsuma, D.M. Mittleman, *Nat. Electron.* **1** No 12, 622 (2018) https://doi.org/10.1038/s41928-018-0173-2.
3. R.A. Lewis, *J. Phys. D: Appl. Phys.* **47** No 37, 374001 (2014) https://doi.org/10.1088/0022-3727/47/37/374001.
4. V. Gružinskis, E. Starikov, P. Shiktorov, *Lith. J. Phys.* **54** No 1, 7 (2014) https://doi.org/10.3952/physics.v54i1.2836.
5. S.P. Khanna et al., *J. Phys. D: Appl. Phys.* **43** No 22, 225101 (2010) https://doi.org/10.1088/0022-3727/43/22/225101.
6. H. Eisele, R. Kamoua, *IEEE Trans. Microw. Theory Technol.* **52** No 10, 2371 (2004) https://doi.org/10.1109/TMTT.2004.835974.
7. H. Eisele, *IEEE Microwave Wireless Compon. Lett.* **19** No 6, 416 (2009) https://doi.org/10.1109/LMWC.2009.2020044.

8. O.V. Botsula, K.H. Prykhodko, *J. Nano- Electron. Phys.* **11** No 2, 02009 (2019) https://doi.org/10.21272/jnep.11(2).02009.
9. I.P. Storozhenko, M.V. Kaydash, *Telecommun. Radio Eng.* **75** No 16, 1495 (2016) https://doi.org/10.1615/TelecomRadEng.v75.i16.70.
10. Khalid, et al., *J. Appl. Phys.* **115** No 11, 114502 (2014) https://doi.org/10.1063/1.4868705.
11. Bin Li et al., *Int. J. Hydrogen Energy* **41** No 35, 15772 (2016) https://doi.org/10.1016/j.ijhydene.2016.04.055.
12. Storozhenko, *J. Nano- Electron. Phys.* **12** No 1, 01015 (2020) https://doi.org/10.21272/jnep.12(1).01015.
13. S. Perez et al., *J. Appl. Phys.* **103** No 9, 094516 (2008) https://doi.org/10.1063/1.2917246.
14. K.H. Prykhodko, O.V. Botsula, *J. Nano- Electron. Phys.* **15** No 6, 06019 (2023) https://doi.org/10.21272/jnep.15(6).06019.
15. A. Dobrinsky et al., *ECS Trans.* **58** No 4, 129 (2013) http://dx.doi.org/10.1149/05804.0129ecst.
16. Yue Hao, Lin-An Yang, Jin-Cheng Zhang, *Int. J. Terahertz Sci. Technol.* **1** No 2, 51 (2008) https://doi.org/10.11906/TST.051-064.2008.06.07.
17. I.P. Storozhenko, Yu.V. Arkusha, *Telecommun. Radio Eng.* **71** No 8, 717 (2012) http://dx.doi.org/10.1615/TelecomRadEng.v71.i8.40.
18. Linan Yang et al., *J. Appl. Phys.* **111** No 10, 104514 (2012) https://doi.org/10.1063/1.4721667.
19. G. Aloise, S. Vitanov, V. Palankovski, *NSTI Nanotechnology Conference and Expo (NSTI-Nanotech 2011)*, 2, 599 (Boston: NSTI: 2011).
20. R.F. Macpherson, G.M. Dunn, N.J. Pilgrim, *Semicond. Sci. Technol.* **23** No 5, 055005, (2008) https://doi.org/10.1088/0268-1242/23/5/055005.
21. M. Farahmand et al., *IEEE Trans. Electron Dev.* **48** No 3, 535 (2001) https://doi.org/10.1109/16.906448.
22. Javier Mateos et al., *2019 IEEE Asia-Pacific Microwave Conference (APMC)*, 971 (Singapore: IEEE: 2019) https://doi.org/10.1109/APMC46564.2019.9038486.
23. Sergio García-Sánchez et al., *IEEE Trans. Electron Dev.* **71** No 10, 5901 (2024) https://doi.org/10.1109/TED.2024.3438114.
24. Ying Wang et al., *IEEE J. Electron Dev. Soc.* **13**, 145 (2025) https://doi.org/10.1109/JEDS.2025.3543017.
25. A. Iniguez-de-la-Torre et al., *J. Appl. Phys.* **111** No 11, 113705 (2012) https://doi.org/10.1063/1.4724350.
26. Ahid S. Hajo et al., *IEEE 45th International Conference on Infrared, Millimeter and Terahertz Waves (IRMMW-THz)*, 978 (Buffalo, NY: IEEE: 2020) https://doi.org/10.1109/IRMMW-THz46771.2020.9370977.
27. V.O. Zozulia et al., *J. Nano- Electron. Phys.* **18** No 1, 01026 (2026) https://doi.org/10.21272/jnep.18(1).01026.
28. Lin'an Yang et al., *J. Appl. Phys.* **109** No 2, 024503 (2011) https://doi.org/10.1063/1.3533984.
29. O. Yilmazoglu, K. Mutamba, D. Pavlidis, T. Karaduman, *IEEE Trans. Electron Dev.* **55** No 6, 1563 (2008) https://doi.org/10.1109/TED.2008.921253.
30. O.V. Botsula, K.H. Prykhodko, *IEEE Ukrainian Microwave Week (UkrMW)*, 3, 925 (Kharkiv: IEEE: 2020) https://doi.org/10.1109/UkrMW49653.2020.9252763.
31. I.P. Storozhenko, *Telecommun. Radio Eng.* **59** No 1-2, 100 (2003) https://doi.org/10.1615/TelecomRadEng.v59.i12.100.
32. J. Zhang, N.G. Anderson, K.M.Lau, *J. Appl. Lett.* **83** No 2, 374 (2003) https://doi.org/10.1063/1.1591242.
33. E. Bellotti et al., *J. Appl. Phys.* **85** No 2, 916 (1999) https://doi.org/10.1063/1.369211.

InN-діоди Ганна субміліметрового діапазону з варізонним GaInN-інжектором

І. Стороженко[1], П. Сіренко[2]

[1] *Державний біотехнологічний університет, 61002 Харків, Україна*
[2] *Ризький університет імені Страдіня, LV-1007 Рига, Латвія*

Розробка ефективних твердотільних джерел субміліметрового діапазону хвиль є ключовим викликом для напівпровідникової електроніки. У цій роботі представлено теоретичне дослідження високочастотних коливань у субмікронних діодах Ганна на основі InN із градієнтним за складом інжектором GaInN поблизу катода. У дослідженні використано тридолинну гідродинамічну модель перенесення електронів, адаптовану для варізонних III-нітридних структур з урахуванням параметрів, що залежать від координати. Ця модель інтегрована в самоузгоджену систему, яка пов'язує рівняння приладу з еквівалентним резонансним контуром і рівнянням Пуассона. На відміну від короткострокового моделювання, цей підхід аналізує стабільну генерацію протягом тисяч циклів, забезпечуючи реалістичні оцінки ВЧ-потужності, ККД та перехідних процесів. Результати показують, що варізонний інжектор GaInN суттєво модифікує динаміку хвиль просторового заряду, сприяючи переходу від дрейфу шару накопичення до нестійкості дипольного домену. Моделювання демонструє, що оптимізація довжини та складу області GaInN суттєво знижує порогову концентрацію електронів для виникнення нестійкості струму. Виявлено специфічний режим «неповного дрейфу домену», за якого шари просторового заряду розсмоктуються в активній області, не досягаючи анода. Це забезпечує частоти до 391 ГГц у приладі довжиною 1,0 мкм, що перевищує основні частоти гомогенних InN-структур. Діод із шаром GaInN товщиною 0,2 мкм забезпечує пікову потужність 116,8 мВт на частоті 300,7 ГГц, що на порядки перевищує показники існуючих приладів на основі InGaAs та InP. У статті також розглядаються проблеми технологічної реалізації, управління температурою та ризик ударної іонізації. Продемонстровано, що діоди на основі InN з інжектором GaInN потенційно можуть бути використані для досягнення коливань у діапазоні суб-ТГц діапазоні.

Ключові слова: Діод Ганна, Прилади на міждолинному перенесенні електронів, Варізонний напівпровідник, нітрид індію, ТГц-діапазон, GaInN інжектор, Гарячі електрони, Домени об'ємного заряду, НДО, Власні коливання.